Design of QMF banks based on derivative information

M.-C.Kao and S.-G.Chen

Abstract: New l_2 objective functions for the design of quadrature mirror filter (QMF) banks are proposed. They are based on the derivative information of the reconstruction error. Simple and explicit matrix-form formulas for the proposed objective functions are derived. Efficient design methods are proposed by incorporating a separability technique into the derived optimality conditions on prototype filters. The proposed design methods need only solve linear equation iteratively without nonlinear optimisation. Design examples demonstrate that good low-delay QMF banks and linear-phase QMF banks can be obtained in only a few iterations. Compared with the conventional approach, the new approach leads to QMF banks with larger stopband attenuation and smaller reconstruction errors.

1 Introduction

Quadrature mirror filter (QMF) banks have a wide range of applications in subband coding and adaptive filtering [1–4]. The underlying issues [1] commonly encountered in QMF banks design include imposing constraints on the frequency characteristics of individual analysis and synthesis filters, and on the reconstruction fidelity of the combined analysis/synthesis system. Various studies have been devoted to the design subject in recent years [1–16].

One very popular type of two-channel QMF bank, which is the focus of this study, involves the design by frequency modulation of a prototype baseband analysis filter $H_0(z)$ [1]. More precisely, the modulated analysis and synthesis filters of Fig. 1 are given by $H_1(z)=H_0(-z)$, $G_0(z)=2H_0(z)$, and $G_1(z)=-2H_0(-z)$. Accordingly, the filtering performance of the QMF bank hinges on the prototype filter $H_0(z)$. Many design techniques for prototype filters had been proposed [10–14], most devoted to linear-phase QMF bank design. They minimise the conventional objective function

$$\Phi_{\text{con}} = \Phi_{\text{d,con}} + \alpha\Phi_{\text{s}} \tag{1}$$

where $\Phi_{\text{d,con}}$, the distortion energy of the overall QMF bank frequency response, is defined as

$$\Phi_{\text{d,con}} = \int_0^{\pi} \left(\left|H_0(e^{j\omega})\right|^2 + \left|H_0(e^{j(\omega+\pi)})\right|^2 - 1\right)^2 d\omega \tag{2}$$

and Φ_{s}, the stopband energy of the prototype filter, is defined as

$$\Phi_{\text{s}} = \int_{\omega_s}^{\pi} \left|H_0(e^{j\omega})\right|^2 d\omega \tag{3}$$

with ω_s being the stopband cutoff frequency of $H_0(z)$. (For simplicity, the subscript 0 of $H_0(z)$ is dropped in the ensuing discussion.) The stopband weight α is a positive number that controls the relative significance of these two errors. Note that normally the passband error is not included in the objective function. The reason [1] is that if the objective function, in terms of the reconstruction error and the stopband error, is minimised the passband error is also reduced accordingly. Therefore the design techniques mentioned did not consider the passband cutoff frequency ω_p. The QMF bank design problem is formulated as an unconstrained nonquadratic minimisation problem that is difficult to solve analytically.

Johnston [11] proposed a search algorithm by using a nonlinear programming optimisation technique. However, such nonlinear optimisation is very complicated. Besides, this algorithm is sensitive to initial values and requires significant manual intervention during the filter optimisation process. Chen and Lee [12] proposed an iterative algorithm by incorporating a linearisation technique to reformulate the fourth-order conventional objective function in a quadratic form. For better performance, however, this algorithm requires higher-density discretisation of frequency grid points at each iteration and is thus also very computation-intensive. Recently, Xu, Lu, and Antoniou [13] improved the algorithm to reduce the computational effort by replacing inexact integral discretisation with exact integration. On the other hand, Jain and Crochiere [14] described a time-domain approach. However, it involves a large amount of computation for the eigendecomposition operations at each iteration, particularly for long filters. In summary, almost all the studies had been devoted to this particular type of objective function rather than to developing new objective functions.

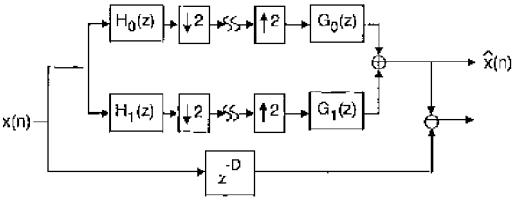

Fig. 1 *Two-channel analysis/synthesis QMF bank and error system*

IEE Proceedings online no. 19990608

DOI: 10.1049/ip-vis:19990608

Paper first received 9th January 1998 and in final revised form 17th February 1999

The authors are with the Department of Electronics Engineering and Institute of Electronics, National Chiao Tung University, Hsinchu, Taiwan, Republic of China

Nonetheless, an appropriate objective function is crucial to the development of a good QMF bank design method.

In this paper, new objective functions that utilise the derivative information of the reconstruction error in the z-domain are proposed. The motivation for using the derivative form (w.r.t. z of the reconstruction error) is as follows. L_2 norm minimisation of the reconstruction error often results in total system magnitude responses that exhibit ripples around ideal value one. It is natural to expect that more error ripples result in larger derivative values of the error ripples. Therefore one would expect that the resulting system responses would be closer to the ideal ones if one can reduce the derivative values of the error ripples. Although the L_2 norm minimisation of the reconstruction error is well documented in the literature, it is not closely related to the minimisation of the derivative of the reconstruction error. Hence, it is interesting to investigate the design results by minimising the derivative information of the reconstruction error.

Another crucial issue of QMF bank design is to have low-delay property, particularly in time critical applications. A low-delay QMF bank refers to a causal QMF bank with a reconstruction delay of $D < N - 1$, in contrast to the fixed delay $D = N - 1$ of a causal linear-phase QMF bank, where N is the length of the prototype filter. In the past, almost all the attention had been given to linear-phase QMF bank design [8, 9]. However, one recognised restriction with linear-phase QMF banks is that its system delay is completely determined by the lengths of the analysis and synthesis filters. One has to make tradeoff between the two conflicting conditions of low system delay and small reconstruction error. Thus, the linear-phase constraint for filters should be relaxed to allow more freedom in designing low-delay QMF banks. Extensions of the mentioned methods [13, 15] to low-delay QMF bank design are straightforward but bear the same problems as they have in linear-phase QMF bank design. In general, studies on low-delay QMF bank design are few [15, 16], and the optimum design method has not been found yet, particularly with equal-length filters.

Based on the proposed objective functions, prototype filter design techniques for low-delay QMF banks and linear-phase QMF banks are developed. Compared with the conventional approach, the proposed approach leads to QMF banks with larger stopband attenuation and smaller reconstruction errors.

2 New objective functions

For good coding efficiency and high-fidelity reconstruction of the QMF bank with D system delays, the causal FIR prototype filter $H(z)$ is required to satisfy the following two conditions:

$$\left|H(e^{j\omega})\right| = 0, \quad \text{for } 0.5\pi < \omega < \pi \tag{4}$$

and

$$H^2(z) - H^2(-z) = z^{-D} \tag{5}$$

where D is an odd number. Here, particularly we are going to investigate two questions: Could the differentiation of eqn. 5 be well approximated by numeric optimisation? Could the resulting QMF bank have smaller reconstruction error than the one resulting from the conventional objective function? The answers are detailed as follows.

By definition, the reconstruction error $E_{con}(z)$ is given as

$$E_{con}(z) = H^2(z) - H^2(-z) - z^{-D} \tag{6}$$

Let the z-domain error term $E_{new,n}(z)$ in its general form, corresponding to the nth derivative of $E_{con}(z)$ with respect to z, be

$$E_{new,n}(z) = \frac{(-z)^n}{D(D+1)\cdots(D+n-1)} \times \frac{d^n}{dz^n}\left\{H^2(z) - H^2(-z)\right\} - z^{-D} \tag{7}$$

The new objective function in its general form is defined to be a weighted sum of the L_2 norms of the specific error $E_{new,n}(z)$ and the stopband ripple as

$$\begin{aligned}\Phi_{new,n} &= \int_0^{\pi} \left|E_{new,n}(e^{j\omega})\right|^2 d\omega + \alpha \int_{\omega_s}^{\pi} \left|H(e^{j\omega})\right|^2 d\omega \\ &= \Phi_{d,n} + \alpha\Phi_s\end{aligned} \tag{8}$$

Varying n leads to different $\Phi_{new,n}$ and QMF banks. In particular, this paper investigates the special cases of the first derivative ($n = 1$) and the second derivative ($n = 2$). Their overall QMF bank frequency responses and filter responses are investigated and compared with those obtained by the conventional function Φ_{con} later. We denote Φ_{new1} and Φ_{new2} as the objective functions corresponding to the first and second derivatives, respectively.

3 Parametrisation and formulation of new objective functions

Let $\boldsymbol{h}$, the filter vector of $H(z)$, be defined as

$$\boldsymbol{h} = \begin{bmatrix} h(0) & h(1) & h(2) & \dots & h(N-1) \end{bmatrix}^T \tag{9}$$

where the superscript $[\,]^T$ stands for the transpose. Then

$$H(z) = \boldsymbol{h}^T \begin{bmatrix} 1 & z^{-1} & z^{-2} & \dots & z^{-(N-1)} \end{bmatrix}^T \tag{10}$$

In particular, the frequency response $H(e^{j\omega})$ can be written as

$$H(e^{j\omega}) = \boldsymbol{h}^T \left\{\boldsymbol{cs}(\omega) - j\boldsymbol{sn}(\omega)\right\} \tag{11}$$

where

$$\boldsymbol{cs}(\omega) = \begin{bmatrix} 1 & \cos(\omega) & \cos(2\omega) & \dots & \cos((N-1)\omega) \end{bmatrix}^T \tag{12a}$$

$$\boldsymbol{sn}(\omega) = \begin{bmatrix} 0 & \sin(\omega) & \sin(2\omega) & \dots & \sin((N-1)\omega) \end{bmatrix}^T \tag{12b}$$

Moreover, $H^2(z)$ can be put in the following matrix product form

$$H^2(z) = (\boldsymbol{Hh})^T \begin{bmatrix} 1 & z^{-1} & z^{-2} & \dots & z^{-(2N-2)} \end{bmatrix}^T \tag{13}$$

where $\boldsymbol{H}$ is a $(2N-1)\times N$ Toeplitz matrix that represents the convolution with $\boldsymbol{h}$

$$\boldsymbol{H} = \begin{bmatrix} h(0) & 0 & 0 & 0 \\ h(1) & h(0) & 0 & 0 \\ \vdots & h(1) & h(0) & 0 \\ \vdots & \vdots & h(1) & h(0) \\ h(N-1) & \vdots & \vdots & h(1) \\ 0 & h(N-1) & \vdots & \vdots \\ 0 & 0 & h(N-1) & \vdots \\ 0 & 0 & 0 & h(N-1) \end{bmatrix} \tag{14}$$

Next, simple and explicit forms for the proposed objective functions can be derived as follows. First, substituting eqn. 13 into eqn. 7 yields

$$E_{\text{new},n}(z) = z^{-D}\left\{2(\boldsymbol{H}\boldsymbol{h})^T \frac{\boldsymbol{\Lambda}(\boldsymbol{\Lambda}+\boldsymbol{I})\cdots(\boldsymbol{\Lambda}+(n-1)\boldsymbol{I})}{D(D+1)\cdots(D+n-1)}\boldsymbol{B}(z) - 1\right\} \tag{15}$$

where

$$\boldsymbol{B}(z) = \begin{bmatrix} 0 & z^{D-1} & 0 & z^{D-3} & \cdots & 0 & z^{D-(2N-3)} & 0 \end{bmatrix}^T,$$

$\boldsymbol{\Lambda}$ and $\boldsymbol{I}$ are $(2N-1)\times(2N-1)$ diagonal matrices given by

$$\boldsymbol{\Lambda} = \mathbf{diag}\begin{bmatrix} 0 & 1 & 0 & 3 & \cdots & 0 & 2N-3 & 0 \end{bmatrix}$$

and

$$\boldsymbol{I} = \mathbf{diag}\begin{bmatrix} 1 & 1 & 1 & 1 & \cdots & 1 & 1 \end{bmatrix},$$

respectively. In particular, there holds

$$\left|E_{\text{new},n}(e^{j\omega})\right| = \left|2(\boldsymbol{H}\boldsymbol{h})^T \frac{\boldsymbol{\Lambda}(\boldsymbol{\Lambda}+\boldsymbol{I})\cdots(\boldsymbol{\Lambda}+(n-1)\boldsymbol{I})}{D(D+1)\cdots(D+n-1)} \times \{\boldsymbol{c}(\omega)+j\boldsymbol{s}(\omega)\} - 1\right| \tag{16}$$

where both $\boldsymbol{c}(\omega)$ and $\boldsymbol{s}(\omega)$ are vectors of size $(2N-1)\times 1$ given by

$$\boldsymbol{c}(\omega) = \begin{bmatrix} 0 & \cos((D-1)\omega) & 0 & \cos((D-3)\omega) & \cdots & 1 & \cdots & \cos((D-2N+3)\omega) & 0 \end{bmatrix}^T \tag{17a}$$

$$\boldsymbol{s}(\omega) = \begin{bmatrix} 0 & \sin((D-1)\omega) & 0 & \sin((D-3)\omega) & \cdots & 0 & \cdots & \sin((D-2N+3)\omega) & 0 \end{bmatrix}^T \tag{17b}$$

After some manipulation, the error term $\Phi_{\text{d},n}$ can be formulated as

$$\Phi_{\text{d},n} = 4(\boldsymbol{H}\boldsymbol{h})^T \frac{\boldsymbol{\Lambda}(\boldsymbol{\Lambda}+\boldsymbol{I})\cdots(\boldsymbol{\Lambda}+(n-1)\boldsymbol{I})}{D(D+1)\cdots(D+n-1)} \times \left(\boldsymbol{Q}_{\text{d}}\frac{(\boldsymbol{\Lambda}+(n-1)\boldsymbol{I})\cdots(\boldsymbol{\Lambda}+\boldsymbol{I})\boldsymbol{\Lambda}}{(D+n-1)\cdots(D+1)D}\boldsymbol{H}\boldsymbol{h} - \boldsymbol{v}\right) + \pi \tag{18}$$

where $\boldsymbol{v}$ is a vector of size $(2N-1)\times 1$ given by

$$\boldsymbol{v} = \begin{bmatrix} 0 & 0 & \cdots & \pi & \cdots & 0 \end{bmatrix}^T$$

with the only nonzero value π in the $(D+1)$th entry, and $\boldsymbol{Q}_{\text{d}}$ is a $(2N-1)\times(2N-1)$ diagonal matrix given by

$$\boldsymbol{Q}_{\text{d}} = \mathrm{diag}\begin{bmatrix} 0 & \pi & 0 & \pi & \cdots & 0 & \pi & 0 \end{bmatrix}$$

It remains to derive the explicit form for the stopband ripple energy Φ_{s}. By substituting eqn. 11 for $H(e^{j\omega})$, Φ_{s} can be formulated as

$$\Phi_{\text{s}} = \boldsymbol{h}^T\boldsymbol{Q}_{\text{s}}\boldsymbol{h} \tag{19}$$

where $\boldsymbol{Q}_{\text{s}}$ is an $N\times N$ symmetric matrix with its (i,j)th entry given by

$$\boldsymbol{Q}_{\text{s}}(i,j) = \begin{cases} -\dfrac{1}{|i-j|}\sin\{|i-j|\omega_s\}, & \text{if } i\neq j,\ i,j = 1\ldots N \\ \pi - \omega_s, & \text{if } i = j,\quad i = 1\ \ldots\ N \end{cases} \tag{20}$$

Consequently, a new objective function $\Phi_{\text{new},n}$ can be formulated explicitly in terms of $\boldsymbol{h}$ and $\boldsymbol{H}$ as

$$\begin{aligned} \Phi_{\text{new},n} = {} & 4(\boldsymbol{H}\boldsymbol{h})^T \frac{\boldsymbol{\Lambda}(\boldsymbol{\Lambda}+\boldsymbol{I})\cdots(\boldsymbol{\Lambda}+(n-1)\boldsymbol{I})}{D(D+1)\cdots(D+n-1)} \\ & \times \boldsymbol{Q}_{\text{d}}\frac{(\boldsymbol{\Lambda}+(n-1)\boldsymbol{I})\cdots(\boldsymbol{\Lambda}+\boldsymbol{I})\boldsymbol{\Lambda}}{(D+n-1)\cdots(D+1)D}\boldsymbol{H}\boldsymbol{h} \\ & - 4(\boldsymbol{H}\boldsymbol{h})^T \frac{\boldsymbol{\Lambda}(\boldsymbol{\Lambda}+\boldsymbol{I})\cdots(\boldsymbol{\Lambda}+(n-1)\boldsymbol{I})}{D(D+1)\cdots(D+n-1)} \\ & \times \boldsymbol{v} + \alpha\boldsymbol{h}^T\boldsymbol{Q}_{\text{s}}\boldsymbol{h} + \pi \end{aligned} \tag{21}$$

The conventional objective function Φ_{con} can be written as

$$\Phi_{\text{con}} = 4(\boldsymbol{H}\boldsymbol{h})^T\boldsymbol{Q}_{\text{d}}\boldsymbol{H}\boldsymbol{h} - 4(\boldsymbol{H}\boldsymbol{h})^T\boldsymbol{v} + \alpha\boldsymbol{h}^T\boldsymbol{Q}_{\text{s}}\boldsymbol{h} + \pi \tag{22}$$

As a result, a generalised objective function can be defined as

$$\Phi = 4(\boldsymbol{H}\boldsymbol{h})^T\boldsymbol{W}^T\boldsymbol{Q}_{\text{d}}\boldsymbol{W}\boldsymbol{H}\boldsymbol{h} - 4(\boldsymbol{H}\boldsymbol{h})^T\boldsymbol{W}^T\boldsymbol{v} + \alpha\boldsymbol{h}^T\boldsymbol{Q}_{\text{s}}\boldsymbol{h} + \pi \tag{23}$$

where

$$\boldsymbol{W} = \begin{cases} \boldsymbol{I}, & \text{if } \Phi = \Phi_{\text{con}} \\ \dfrac{(\boldsymbol{\Lambda}+(n-1)\boldsymbol{I})\cdots(\boldsymbol{\Lambda}+\boldsymbol{I})\boldsymbol{\Lambda}}{(D+n-1)\cdots(D+1)D}, & \text{if } \Phi = \Phi_{\text{new},n} \end{cases} \tag{24}$$

As shown, $\Phi_{\text{new},n}$ provides an additional weighting matrix $\boldsymbol{W}$ to the characteristic matrix $\boldsymbol{Q}_{\text{d}}$ and vector $\boldsymbol{v}$, in contrast to the nonweighted Φ_{con}. The weighting matrix $\boldsymbol{W}$ relates primarily to the delay parameter D.

4 Optimisation of new objective functions and design of QMF banks

An efficient method is developed for finding the optimal filter vector. This method is in essence an iterative procedure that makes the filter vector descend to the minimum of the objective function. The design procedure only needs to solve a set of linear equations iteratively without nonlinear optimisation. Convergence of the design procedure occurs in a few iterations.

4.1 Design of QMF banks

Let $\boldsymbol{h}_{opt,n}$ be the optimal prototype filter at which $\Phi_{\text{new},n}$ attains its minimum. The minimisation of this error is

achieved when $\nabla_h \Phi_{\text{new},n} = \mathbf{0}$. Consequently, the optimality condition on $\boldsymbol{h}_{opt,n}$ becomes as

$$\left(8(\boldsymbol{H}_{opt,n})^T \frac{\Lambda(\Lambda+\boldsymbol{I})\ldots(\Lambda+(n-1)\boldsymbol{I})}{D(D+1)\ldots(D+n-1)} \times \boldsymbol{Q}_d \frac{(\Lambda+(n-1)\boldsymbol{I})\ldots(\Lambda+\boldsymbol{I})\Lambda}{(D+n-1)\ldots(D+1)D} \boldsymbol{H}_{opt,n} + \alpha \boldsymbol{Q}_s\right)\boldsymbol{h}_{opt,n} = 4(\boldsymbol{H}_{opt,n})^T \frac{\Lambda(\Lambda+\boldsymbol{I})\ldots(\Lambda+(n-1)\boldsymbol{I})}{D(D+1)\ldots(D+n-1)}\boldsymbol{v} \tag{25}$$

where $\boldsymbol{H}_{opt,n}$ is the Toeplitz matrix that corresponds to $\boldsymbol{h}_{opt,n}$. This system of equations is hard to solve owing to its high nonlinearity. An efficient way to approach $\boldsymbol{h}_{opt,n}$ is by separating the unknown vector $\boldsymbol{h}$ from the available matrix $\boldsymbol{H}$ at each iteration and by iterating through the following two steps:

(i) form a fixed $\boldsymbol{H}$ from the newly obtained $\boldsymbol{h}$
(ii) solve the following set of linear equations

$$\left(8\boldsymbol{H}^T \frac{\Lambda(\Lambda+\boldsymbol{I})\ldots(\Lambda+(n-1)\boldsymbol{I})}{D(D+1)\ldots(D+n-1)} \times \boldsymbol{Q}_d \frac{(\Lambda+(n-1)\boldsymbol{I})\ldots(\Lambda+\boldsymbol{I})\Lambda}{(D+n-1)\ldots(D+1)D} \boldsymbol{H} + \alpha \boldsymbol{Q}_s\right)\boldsymbol{h} = 4\boldsymbol{H}^T \frac{\Lambda(\Lambda+\boldsymbol{I})\ldots(\Lambda+(n-1)\boldsymbol{I})}{D(D+1)\ldots(D+n-1)}\boldsymbol{v} \tag{26}$$

and update $\boldsymbol{h}$ by linearly combining $\boldsymbol{h}$ and the solution of eqn. 26. The iterative procedure may be terminated when the new solution is within a relatively small deviation from the current solution.

Note that the separability technique incorporated in the proposed iterative algorithms is different from the linearisation technique in the literature [12–14]. Actually, the separability technique transforms the QMF bank optimisation problem into a convergent fixed-point problem, simply by algebraically separating the vector variable $\boldsymbol{h}$ from a system of nonlinear equations. The proposed two-step procedure is a functional iteration scheme of the form $\boldsymbol{h}_n = \boldsymbol{G}(\boldsymbol{h}_{n-1})$, where $\boldsymbol{G}(\boldsymbol{h}_{n-1}) = \boldsymbol{h}_{n-1} - \boldsymbol{F}(\boldsymbol{h}_{n-1})$, which is simple and efficient for our design purpose. Unlike many popular optimisation techniques, the optimisation procedure does not involve search steps and nonlinear optimisation. Like the more complicated Newton's method, the procedure converges fairly fast once an approximation near the true solution is obtained. Generally, the procedure gives linear convergence. In our simulations it took only a few iterations (see tables) to converge, depending on the filter length. On the other hand, Newton's method for nonlinear systems is a functional iteration scheme of the form $\boldsymbol{h}_n = \boldsymbol{G}(\boldsymbol{h}_{n-1})$, where $\boldsymbol{G}(\boldsymbol{h}_{n-1}) = \boldsymbol{h}_{n-1} - \boldsymbol{J}(\boldsymbol{h}_{n-1})^{-1}\boldsymbol{F}(\boldsymbol{h}_{n-1})$. Generally, Newton's method gives quadratic convergence, provided that a sufficiently accurate initial point is known and the Jacobian matrix $\boldsymbol{J}(\boldsymbol{h})$ is nonsingular at the fixed point to be converged. However, Newton's method requires evaluation of $\boldsymbol{J}(\boldsymbol{h}_n)$ at each step, and is more expensive to employ.

For $\Phi = \Phi_{\text{con}}$, $\boldsymbol{h}_{opt,\text{con}}$ can be solved similarly and the required set of linear equations is

$$\left(8\boldsymbol{H}^T\boldsymbol{Q}_d\boldsymbol{H} + \alpha\boldsymbol{Q}_s\right)\boldsymbol{h} = 4\boldsymbol{H}^T\boldsymbol{v} \tag{27}$$

The design algorithm is summarised as follows.

(i) Specify the filter length N, stopband cutoff frequency ω_s, system delay D, stopband weight α, smoothing value τ $(0 < \tau < 1)$, and relative error tolerance ε.

(ii) Select an initial filter $\boldsymbol{h}_0$ by using any available FIR filter design method. Set the iteration index $i = 0$.
(iii) Construct $\boldsymbol{H}_i$ from $\boldsymbol{h}_i$.
(iv) Compute $\boldsymbol{h}^*$ from the following design formula:

$$\boldsymbol{h}^* = \begin{cases} 4(8(\boldsymbol{H}_i)^T\boldsymbol{Q}_d\boldsymbol{H}_i + \alpha\boldsymbol{Q}_s)^{-1}(\boldsymbol{H}_i)^T\boldsymbol{v}, & \text{if } \Phi = \Phi_{\text{con}} \\ 4\left(8(\boldsymbol{H}_i)^T \frac{\Lambda(\Lambda+\boldsymbol{I})\ldots(\Lambda+(n-1)\boldsymbol{I})}{D(D+1)\ldots(D+n-1)} \times \boldsymbol{Q}_d \frac{(\Lambda+(n-1)\boldsymbol{I})\ldots(\Lambda+\boldsymbol{I})\Lambda}{(D+n-1)\ldots(D+1)D}\boldsymbol{H}_i + \alpha\boldsymbol{Q}_s\right)^{-1} \\ \quad \times (\boldsymbol{H}_i)^T \frac{\Lambda(\Lambda+\boldsymbol{I})\ldots(\Lambda(\Lambda+(n-1)\boldsymbol{I})}{D(D+1)\ldots(D+n-1)}\boldsymbol{v}, & \text{if } \Phi = \Phi_{\text{new},n} \end{cases}$$

(v) Terminate if $\|\boldsymbol{h}_i - \boldsymbol{h}^*\| < \varepsilon$, otherwise update $\boldsymbol{h}_{i+1}$ by

$$\boldsymbol{h}_{i+1} \leftarrow (1-\tau)\boldsymbol{h}_i + \tau\boldsymbol{h}^*.$$

Set $i = i+1$ and go to (iii).

4.2 Design of linear-phase QMF banks

Consider next the linear-phase case. The prototype filter $H(z)$ is restricted to be of type-2 linear phase (i.e. N is even and $h(n) = h(N-1-n)$). The impulse response can be expressed by

$$\boldsymbol{h} = \begin{bmatrix} \boldsymbol{I}_{\frac{N}{2}} \\ \boldsymbol{J}_{\frac{N}{2}} \end{bmatrix} \boldsymbol{h}_{\text{sym}} = \boldsymbol{K}\boldsymbol{h}_{\text{sym}} \tag{28}$$

where $\boldsymbol{h}_{\text{sym}}$ is the vector consisting of the first half of the $\{h(n)\}$ sequence, $\boldsymbol{I}_{N/2}$ is the $N/2 \times N/2$ identity matrix and $\boldsymbol{J}_{N/2}$ is the $N/2 \times N/2$ exchange matrix. One can obtain the required set of linear equations

$$\left(8(\boldsymbol{H}\boldsymbol{K})^T \frac{\Lambda(\Lambda+\boldsymbol{I})\ldots(\Lambda+(n-1)\boldsymbol{I})}{D(D+1)\ldots(D+n-1)} \times \boldsymbol{Q}_d \frac{(\Lambda+(n-1)\boldsymbol{I})\ldots(\Lambda+\boldsymbol{I})\Lambda}{(D+n-1)\ldots(D+1)D}\boldsymbol{H}\boldsymbol{K} + \alpha\boldsymbol{K}^T\boldsymbol{Q}_s\boldsymbol{K}\right)\boldsymbol{h}_{\text{sym}} = 4(\boldsymbol{H}\boldsymbol{K})^T \frac{\Lambda(\Lambda+\boldsymbol{I})\ldots(\Lambda+(n-1)\boldsymbol{I})}{D(D+1)\ldots(D+n-1)}\boldsymbol{v} \tag{29}$$

when using $\Phi_{\text{new},n}$, and

$$\left(8(\boldsymbol{H}\boldsymbol{K})^T\boldsymbol{Q}_d\boldsymbol{H}\boldsymbol{K} + \alpha\boldsymbol{K}^T\boldsymbol{Q}_s\boldsymbol{K}\right)\boldsymbol{h}_{\text{sym}} = 4(\boldsymbol{H}\boldsymbol{K})^T\boldsymbol{v} \tag{30}$$

when using Φ_{con}. Accordingly, a modified design algorithm is obtained as follows.

(i) Specify N, ω_s, α, τ $(0 < \tau < 1)$, and ε.
(ii) Select a linear-phase filter $\boldsymbol{h}_0$ by using any available FIR filter design method. Set the initial vector $\boldsymbol{h}_{0,\text{sym}}$ to be the first half of the coefficients of $\boldsymbol{h}_0$. Set the iteration index $i = 0$.
(iii) Construct $\boldsymbol{H}_i$ from $\boldsymbol{h}_{i,\text{sym}}$.
(iv) Compute $\boldsymbol{h}^*_{\text{sym}}$ from the following design formula:

$$\boldsymbol{h}^*_{\text{sym}} = \begin{cases} 4(8(\boldsymbol{H}_i\boldsymbol{K})^T\boldsymbol{Q}_d\boldsymbol{H}_i\boldsymbol{K} + \alpha\boldsymbol{K}^T\boldsymbol{Q}_s\boldsymbol{K})^{-1}(\boldsymbol{H}_i\boldsymbol{K})^T\boldsymbol{v}, & \text{if } \Phi = \Phi_{\text{con}} \\ 4\left(8(\boldsymbol{H}_i\boldsymbol{K})^T \frac{\Lambda(\Lambda+\boldsymbol{I})\ldots(\Lambda+(n-1)\boldsymbol{I})}{D(D+1)\ldots(D+n-1)}\boldsymbol{Q}_d \times \frac{(\Lambda+(n-1)\boldsymbol{I})\ldots(\Lambda+\boldsymbol{I})\Lambda}{(D+n-1)\ldots(D+1)D}\boldsymbol{H}_i\boldsymbol{K} + \alpha\boldsymbol{K}^T\boldsymbol{Q}_s\boldsymbol{K}\right)^{-1} \\ \quad \times (\boldsymbol{H}_i\boldsymbol{K})^T \frac{\Lambda(\Lambda+\boldsymbol{I})\ldots(\Lambda+(n-1)\boldsymbol{I})}{D(D+1)\ldots(D+n-1)}\boldsymbol{v}, & \text{if } \Phi = \Phi_{\text{new},n} \end{cases}$$

(v) Terminate if $\|\boldsymbol{h}_{i,\mathrm{sym}} - \boldsymbol{h}^*_{\mathrm{sym}}\| < \varepsilon$, otherwise update $\boldsymbol{h}_{i+1,\mathrm{sym}}$ by

$$\boldsymbol{h}_{i+1,\mathrm{sym}} \leftarrow (1-\tau)\boldsymbol{h}_{i,\mathrm{sym}} + \tau \boldsymbol{h}^*_{\mathrm{sym}}.$$

Set $i = i+1$ and go to (iii).

5 Design examples and comparisons

Three design examples for low-delay QMF banks and linear-phase QMF banks are presented. All of the designs are performed using MATLAB. For convenience, we denote Φ_{new1}-design, Φ_{new2}-design, and Φ_{con}-design as the designs using the objective functions Φ_{new1}, Φ_{new2}, and Φ_{con}, respectively. For comparison of all the designs, the proposed iterative algorithm is applied to minimise all the objective functions including Φ_{con}. The choice of test signals is for the consideration of subjecting all the design methods to extreme inputs. Specifically, they are the better-case narrowband signal and the worse-case wideband signal. As the narrowband test signal, an AR(1) input with correlation factor $\rho = 0.9$ is used. As the wideband test signal, a uniformly distributed random input is used. The length of the test signals is 2^{16}. To generate a uniformly distributed random input, we use the MATLAB function *rand*. This generator can generate all the floating-point numbers in the interval $[2^{-53}, 1-2^{-53}]$. For comparisons among all the designs, the following performance measures are used:

(i) A_a (dB), the minimum attenuation in the stopband of $H(e^{j\omega})$, $A_a = \min_{\omega_s \le \omega \le \pi} \{-20 \log_{10} |H(e^{j\omega})|$.
(ii) A_p (dB), the peak-to-peak passband ripple of $H(e^{j\omega})$ with the passband cutoff frequency ω_p, $A_p = \max_{0 \le \omega \le \omega_p} \{20 \log_{10} |H(e^{j\omega})|\} - \min_{0 \le \omega \le \omega_p} \{20 \log_{10} |H(e^{j\omega})|\}$.
(iii) *AL* (dB), the first sidelobe attenuation in the stopband of $H(e^{j\omega})$.
(iv) *PRE* (dB), the absolute maximum reconstruction error of the QMF bank designed, $PRE = \max_{0 \le \omega \le \pi} \{20 \log_{10} |H^2(e^{j\omega}) + H^2(e^{j(\omega+\pi)}) - e^{-jD\omega}|\}$.
(v) SNR_a (dB) and SNR_r (dB), the signal to reconstruction noise ratios (*SNR*), are due to an AR(1) input $x(n)$ with correlation factor $\rho = 0.9$ and an uniformly distributed random input, respectively, where

$$SNR = 10 \log_{10} \left\{ \frac{\sum x^2(n)}{\sum [x(n) - \hat{x}(n+D)]^2} \right\}.$$

The comparison emphasises the qualities of the resulting prototype filters and QMF banks owing to different objective functions, all obtained by the same new iterative optimisation algorithm. The initial values of the linear-phase prototype filters are obtained by using the Parks–McClellan equiripple filter design method.

5.1 Design example 1

First consider the design of low-delay QMF banks. In this example a delay of 15 is imposed. The design parameters are as follows:

$$N = 32, D = 15, \omega_s = 0.67\pi, \alpha = 0.01,$$
$$\tau = 0.5, \text{ and } \varepsilon = 10^{-3}$$

Table 1 lists the results of performance comparisons among the new and conventional designs. Fig. 2 shows the corresponding amplitude responses of the QMF analysis filters. One can observe that the Φ_{new1}-design shows a good amplitude response with large stopband attenuation. The sidelobe attenuation values are larger than 60 dB. In addition, the Φ_{new1}-design improves A_a by 10.8 dB over the Φ_{con}-design. Similarly, the $\Phi_{\mathrm{new\ 2}}$-design improves A_a by 10.4 dB over the Φ_{con}-design. As shown in Fig. 2, the filter responses of the new designs are better than that of the conventional one. Fig. 3 shows the reconstruction error spectra of the resulting low-delay QMF banks due to those three designs. As shown, both Φ_{new1}-design and Φ_{new2}-design have smaller variations in reconstruction error and smaller *PRE* value than the Φ_{con}-design. Under the error tolerance threshold ε of 10^{-3}, the Φ_{new1}-design, Φ_{new2}-design and Φ_{con}-design need 6, 7 and 10 iterations,

Table 1: Performance comparisons of design example 1

	Φ_{con}	Φ_{new1}	Φ_{new2}
A_a	33.75	**44.52**	44.12
A_p	0.015	**0.002**	0.004
AL	47.50	**54.69**	54.19
PRE	5.59×10^{-4}	$\mathbf{2.19 \times 10^{-4}}$	2.75×10^{-4}
SNR_r	75.6	**79.6**	77.9
SNR_a	74.4	**80.4**	78.7
Iterations	10	**6**	7

$N = 32$; $D = 15$; $\omega_s = 0.67\ \pi$; $\omega_p = 0.35\pi$; $\alpha = 0.01$; $\tau = 0.5$; $\varepsilon = 10^{-3}$

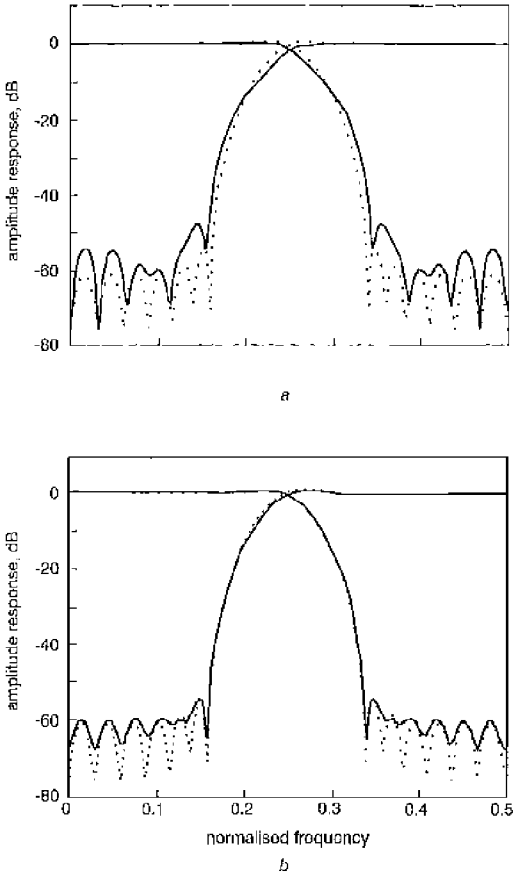

Fig. 2 *Amplitude responses of lowpass and highpass analysis filters for design example 1*
a — Φ_{con} ····· Φ_{new1}
b — Φ_{new2} ····· Φ_{new1}

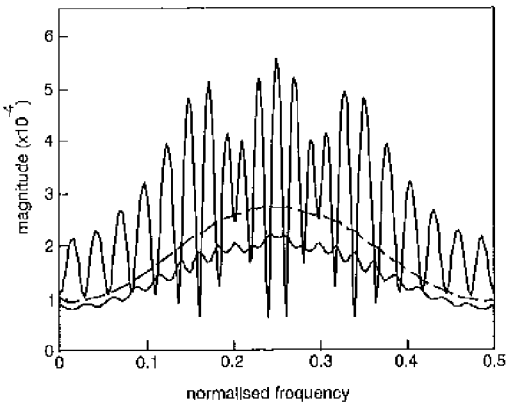

Fig. 3 *Overall reconstruction errors for design example 1*

Φ_{con}
Φ_{new2}
Φ_{new1}

respectively. The design results indicate that the new designs are superior to the conventional design.

5.2 Design example 2

This example illustrates the effect of a wider transition band and a larger stopband weight. Here except that ω_s is 0.69π instead of 0.67π and α is 0.2 instead of 0.01, all the other design parameters are the same as those of design example 1. Table 2 lists the design results. Fig. 4 shows the amplitude responses of the resulting prototype filters. Again, one can observe that the Φ_{new1}-design shows a good amplitude response with large stopband attenuation.

Table 2: Performance comparisons of design example 2

	Φ_{con}	Φ_{new1}	Φ_{new2}
A_a	45.32	**53.01**	52.81
A_p	0.021	**0.004**	0.006
AL	54.42	**61.62**	61.61
PRE	5.51×10^{-4}	$\mathbf{1.57\times10^{-4}}$	1.76×10^{-4}
SNR_r	73.8	**81.5**	79.9
SNR_a	74.8	**81.8**	80.1
Iterations	10	8	**7**

$N=32$; $D=15$; $\omega_s=0.69\,\pi$; $\omega_p=0.35\pi$; $\alpha=0.2$; $\tau=0.5$; $\varepsilon=10^{-3}$

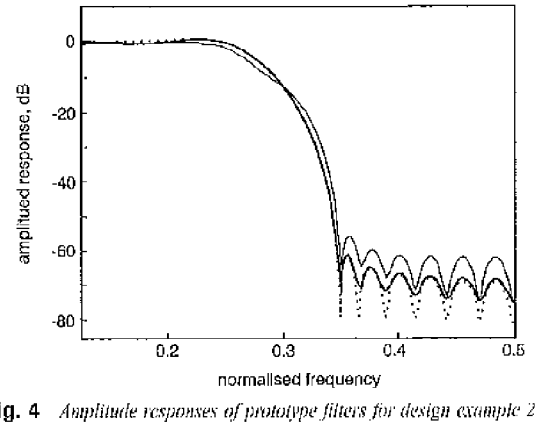

Fig. 4 *Amplitude responses of prototype filters for design example 2*

Φ_{con}
Φ_{new2}
Φ_{new1}

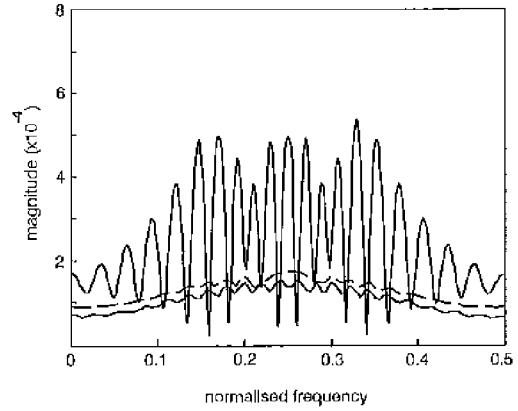

Fig. 5 *Overall reconstruction errors for design example 2*

Φ_{con}
Φ_{new2}
Φ_{new1}

The sidelobe attenuation values are larger than 65 dB. Fig. 5 shows the reconstruction error spectra of the resulting low-delay QMF banks. Again, both Φ_{new1}-design and Φ_{new2}-design have smaller variations in reconstruction error and smaller *PRE* value than the Φ_{con}-design. Compared with the new designs of example 1, the designs with a wider transition band and a larger stopband weight have lower stopband ripples, a larger A_a and a smaller *PRE*.

5.3 Design example 3

Consider the design of linear-phase QMF banks. The design parameters are as follows:

$$N=64,\ \omega_s=0.62\pi,\ \alpha=0.0001,\ \tau=0.5,\ \text{and}\ \varepsilon=10^{-5}$$

Table 3 lists the design results. Figs. 6–8 show that all design approaches produce linear-phase prototype filters with good amplitude responses and large stopband attenuation. All exhibit flatness in the passband and sharp drops in the trailing part of the transition band. The attenuation values at the first sidelobes of the conventional and the proposed designs are all larger than 70 dB. Figs. 9–11 shows that the reconstruction errors of the resulting linear-phase QMF banks are small and similar. Since longer filters provide more parameters to be optimised, reconstruction errors can be made smaller (and more similar) in all design approaches. On the other hand, in cases of linear-phase prototype filters, the weighting matrices $\boldsymbol{W}$ due to proposed design approaches are found to be closer to $\boldsymbol{I}$ of the conventional design approach than the nonlinear phase cases.

Table 3: Performance comparisons of design example 3 (linear-phase QMF bank)

	Φ_{con}	Φ_{new1}	Φ_{new2}
A_a	65.60	65.01	63.10
A_p	5.09×10^{-6}	4.91×10^{-6}	$\mathbf{4.17\times10^{-6}}$
AL	74.09	73.64	71.99
PRE	5.89×10^{-7}	5.65×10^{-7}	$\mathbf{4.76\times10^{-7}}$
SNR_r	130.6	130.8	**132.7**
SNR_a	130.5	130.7	**132.7**
Iterations	24	26	25

$N=64$; $\omega_s=0.62\,\pi$; $\omega_p=0.38\pi$; $\alpha=0.0001$; $\tau=0.5$; $\varepsilon=10^{-5}$

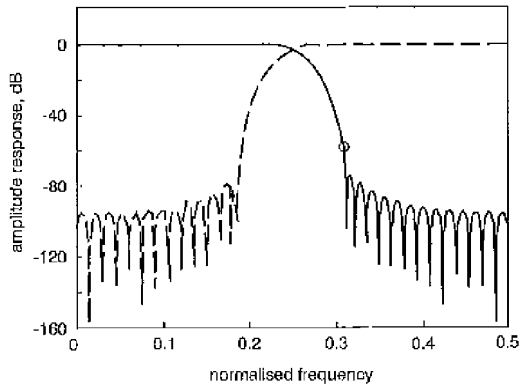

Fig. 6 *Amplitude response of linear-phase lowpass and highpass analysis filters for design example 3: Φ_{con}-design*

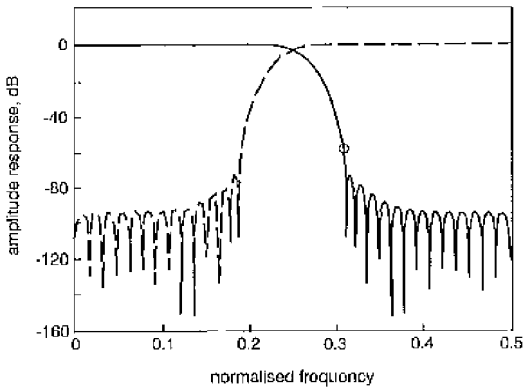

Fig. 7 *Amplitude response of linear-phase lowpass and highpass analysis filters for design example 3: Φ_{new1}-design*

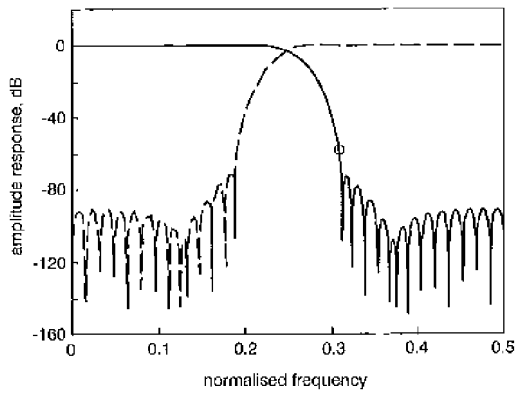

Fig. 8 *Amplitude response of linear-phase lowpass and highpass analysis filters for design example 3: Φ_{new2}-design*

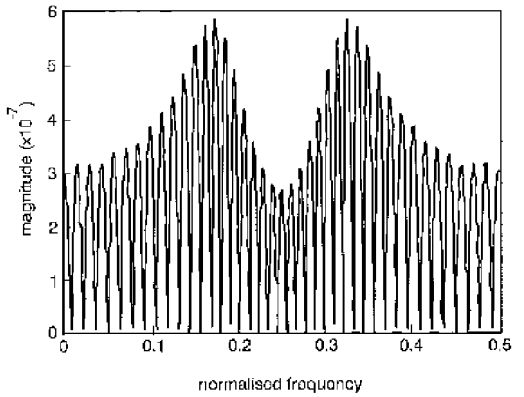

Fig. 9 *Overall reconstruction error for design example 3: Φ_{con}-design*

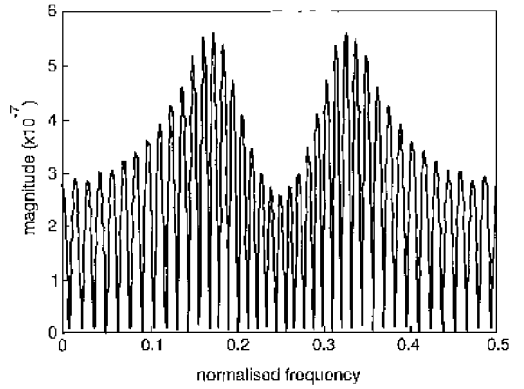

Fig. 10 *Overall reconstruction error for design example 3: Φ_{new1}-design*

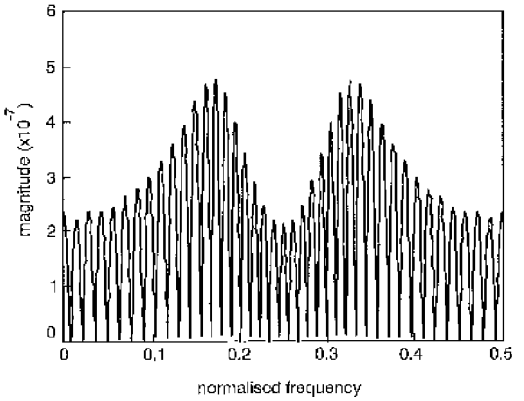

Fig. 11 *Overall reconstruction error for design example 3: Φ_{new2}-design*

Still, there is noticeable difference between the conventional and proposed design approaches, owing to the nonconstant weighting matrix W. From Fig. 8, the Φ_{new2}-design exhibits a dip around 0.75π. Also from Figs. 9–11, the proposed designs have significantly smaller *PRE* value than that of the Φ_{con}-design. The amount of overall reconstruction error is expectedly getting smaller with increasing derivative orders. The results show that the proposed approach has slightly better performance than that of the conventional approach.

6 Conclusions

A new approach to the design of two-channel QMF banks was proposed. Compared with the conventional approach, the approach can yield QMF banks with larger stopband attenuation and smaller reconstruction errors. The improvements are more significant in the low-delay QMF bank cases than in the linear-phase QMF bank cases. The adjustable weighting matrix W suggests possible alternatives and flexibility for designing QMF banks, which deserves further investigation. Moreover, the proposed approach can be extended to the design of two-channel

QMF banks with different weighted $L_p(p > 2)$ error criteria, as well as M-channel ($M > 2$) pseudo-QMF banks.

7 Acknowledgment

This work was supported in part under grant NSC87-2213-E-009-081 of National Science Council, Taiwan.

8 References

1 VAIDYANATHAN, P.P.: 'Multirate systems and filter banks' (Prentice-Hall, Englewood Cliffs, NJ, 1993)
2 GARCIA, C., and RODRIGUEZ, L.: 'Application of a low-delay bank of filters to speech coding'. Proceedings of IEEE workshop on *Digital signal processing*, 1994, pp. 219–222
3 ESTEBAN, D., and GALAND, C.: 'Application of quadrature mirror filter to split-band voice coding schemes'. Proceedings of ICASSP, 1997, pp. 191–195
4 SMITH, M.J.T., and BARNWELL, T.P.: 'Exact reconstruction techniques for tree-structured subband coders', *IEEE Trans. Acoust. Speech Signal Process.*, 1986, **ASSP-34**, (3), pp. 434–441
5 KAO, M.-C., and CHEN, S.-G.: 'A new approach to the design of QMF banks', Proceedings of IEEE international symposium on *Circuits and systems*, ISCAS'98, May 1998, Monterey, CA, USA, TAA1-4
6 CHEN, S.-G., and KAO, M.-C.: 'Low-complexity, perfect reconstruction FIR QMF bank', *Electron. Lett.*, 1998, **34**, pp. 1477–1478
7 CHEN, S.-G., KAO, M.-C., and CHEN, S.-P.: 'A new type of perfect-reconstruction QMF banks'. Proceedings of 30th annual Asilomar conference on *Signals, systems and computers*, 1996, pp. 1334–1338
8 NGUYEN, T.Q., and VAIDYANATHAN, P.P.: 'Two-channel perfect-reconstruction FIR QMF structures which yield linear-phase analysis and synthesis filters', *IEEE Trans. Acoust. Speech Signal Process.*, 1989, **37**, (5), pp. 676–690
9 NGUYEN, T.Q., and VAIDYANATHAN, P.P.: 'Structures for M-channel perfect-reconstruction FIR QMF banks which yield linear-phase analysis filters', *IEEE Trans. Acoust. Speech Signal Process.*, 1990, **38**, (3), pp. 433–446
10 LIM, Y.C., YANG, R.H., and KOH, S.N.: 'The design of weighted minmax quadrature mirror filters', *IEEE Trans. Signal Process.*, 1993, **41**, pp. 1780–1788
11 JOHNSTON, J.D.: 'A filter family designed for use in quadrature mirror filter banks', Proceedings of ICASSP 1980, pp. 291–294
12 CHEN, C.-K., and LEE, J.-H.: 'Design of quadrature mirror filters with linear phase in the frequency domain', *IEEE Trans. Circuits Syst. II, Analog Digit. Signal Process.*, 1992, **39**, (9), pp. 593–605
13 XU, H., LU, W.-S., and ANTONIOU, A.: 'Improved iterative methods for the deign of quadrature mirror-image filter banks', *IEEE Trans. Circuits Syst. II, Analog Digit. Signal Process.*, 1996, **43**, (5), pp. 363–371
14 JAIN, V.K., and CROCHIERE, R.E.: 'Quadrature mirror filter design in the time domain', *IEEE Trans. Acoust. Speech Signal Process.*, 1984, **ASSP-32**, (2), pp. 353–361
15 XU, H., LU, W.-S., and ANTONIOU, A.: 'A new approach for the design of FIR analysis-synthesis filter banks with short reconstruction delays', Proceedings of Canadian conference on *Electron Comp. Eng.*, Sept. 1993, pp. 31–34
16 NAYEBI, K., BARNWELL, T.P., and SMITH, M.J.T.: 'Low delay FIR filter banks: design and evaluation', *IEEE Trans. Signal Process.*, 1994, **42**, (1), pp. 24–31